Electronic Supplementary Material (ESI) for Organic Chemistry Frontiers.

Supporting Information

Efficient Blue Electro-fluorescence Material with High Electron and Balanced Carrier Mobilities Based on Effective π-stacking Between Acceptors

*Mizhen Sun, Chenglin Ma, Mingliang Xie, Lizhi Chu, Xin Wang, Qikun Sun, Wenjun Yang, and Shanfeng Xue**

M. Sun, C. Ma, M. Xie, L. Chu, X. Wang, Q. Sun, Prof. W. Yang, Prof. S. Xue
Key Laboratory of Rubber-Plastics of the Ministry of Education, School of Polymer Science & Engineering, Qingdao University of Science and Technology, Qingdao 266042, P. R. China.
E-mail: sfxue@qust.edu.cn

Contents

SI-1 General Methods

S1.1 Materials

All raw materials involved in the synthesis process were purchased from Aldrich Chemical Co. or Energy Chemical Co., China. The organic and metallic materials for transporting layers in OLEDs fabrication were purchased from P-OLED (Shanghai) Technology CO., LTO. Tetrahydrofuran (THF) was distilled over metallic sodium over calcium hydride before use. The other organic solvents and reagents were all commercially available analytical-grade products and used as received without further purification.

S1.2 Measurements

^{1}H and ^{13}C NMR spectra were recorded on a Mercury 500 spectrometer. MALDI-TOF-MS mass spectra were measured using an AXIMA-CFRTM plus instrument. The dates of thermal gravimetric analysis (TGA) are from Perkin-Elmer thermal analysis system with the temperature of 50-800 °C under a heating rate of 10 °C /min and the nitrogen atmosphere. The dates of Differential scanning calorimetry (DSC) are from NETZSCH (DSC-204) instrument with the temperature of 50-500 °C at a heating rate of 10 °C /min and a nitrogen flow rate of 80 mL/min. UV-vis absorption spectra were measured on a Hitachi U-4100 spectrophotometer. Fluorescence measurements, low temperature fluorescence spectrum and low temperature phosphorescence spectrum were measured on a Hitachi F-4600 spectrophotometer. Cyclic voltammetry (CV) analysis of the materials was recorded on a three-electrode cell with tetra-n-butyl-ammonium hexafluorophosphate (TBAPF6, 0.1 m in acetonitrile) as the supporting electrolyte. Two platinum wires were used as counter electrode and reference electrode. The scan rate is 100 mV/s, and all the potentials were corrected to the ferrocene/ferrocene + (Fc/Fc +) standard under room temperature. The oxidation curve is obtained by dissolving the product and electrolyte in dichloromethane (DCM), and the reduction curve is obtained in N, N-Dimethylformamide (DMF). The lifetimes of solutions were measured on an Edinburgh FLS-980 spectrometer with an EPL-375 optical laser. Photoluminescence quantum yield was recorded using an FLS980 spectrometer.

S1.3 Device fabrication

ITO-coated glass with a sheet resistance of 15-20 Ω square^{-1} was used as the substrate. Before device fabrication, the ITO glass substrates were cleaned with acetone, HellmanexTM III and deionized water, dried 12 h in an oven at 80 °C, the substrates were treated by O_2 plasma for 7 minutes to improve the hole injection ability of ITO. Finally transferred to a vacuum deposition system with a pressure of $< 1.6\times10^{-4}$ Pa. The current-voltage-brightness characteristics were measured by using a Keithley source measurement unit (Keithley 2450 and LS-160), EL spectra

were measured with Flame-S (Serial Number: FLMS16791, Range: > 350 nm). EQEs were calculated from the luminance, current density, and EL spectrum, all the results were measured in the forward-viewing direction without using any light out-coupling technique. The evaporation method for carrier mobility is the same as that for device evaporation, and the testing method is the space charge limited current method (SCLC).

SI-2 Detailed synthesis route

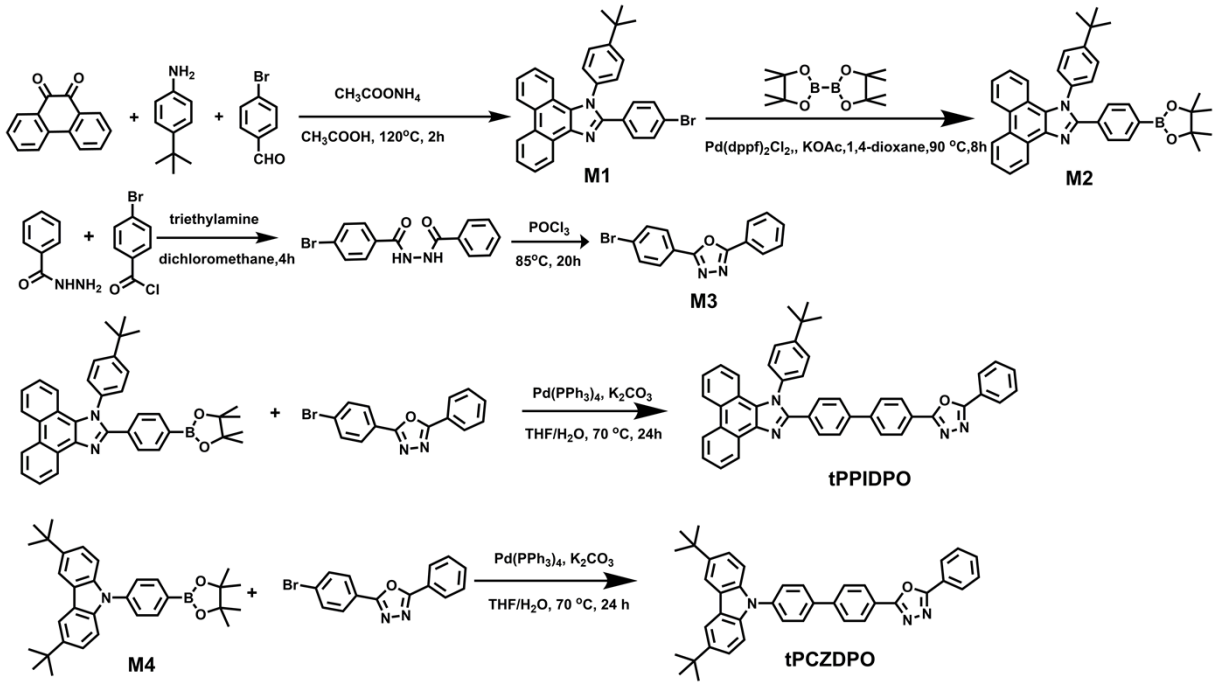

Scheme. S1 Detailed molecular synthesis routes of Tppidpo and tPCZDPO.

Synthesis of 2-(4-bromophenyl)-1-(4-(*tert*-butyl)phenyl)-1*H*-phenanthro[9,10 *d*]imidazole (M1) :

A mixture of phenanthrene-9,10-dione (2.00 g, 9.61 mmol), 4-(*tert*-butyl)aniline (5.74 g, 38.44 mmol), 4-bromobenzaldehyde (1.78 g, 9.61 mmol), ammonium acetate (3.70 g, 48.03 mmol), and acetic acid (30 mL) was refluxed for 2 h under nitrogen. After cooling down, the solid product was filtrated and washed with water/acetic acid (1:1; v/v). The collected solids were dissolved in CH_2Cl_2 and dried in $MgSO_4$, purified by thin layer chromatography, and the white solid product (4.27 g, 88.0 %) was obtained.

Synthesis of 1-(4-(*tert*-butyl)phenyl)-2-(4-(4,4,5,5-tetramethyl-1,3,2 dioxaborolan-2-yl)phenyl)-1*H*-phenanthro[9,10-*d*]imidazole (M2):

A solution of 2-(4-bromophenyl)-1-(4-(*tert*-butyl)phenyl)-1*H*-phenanthro[9,10-*d*]imidazole (4.00 g, 7.91 mmol), 4,4,4',4',5,5,5',5'-octamethyl-2,2'-bi(1,3,2-dioxaborolane) (2.41 g, 9.50 mmol), $PdCl_2$(dppf) (0.17 g, 0.24 mmol) and KOAc (2.33 g, 23.74 mmol) in degassed 1, 4-dioxane (50 mL) was stirred at 90 ℃ for 8 hours. The reaction was quenched by deionized water, and the resulting mixture was washed with dichloromethane. The organic layers were collected, dried with anhydrous magnesium sulphate, and concentrated in vacuum. It was purified via silica gel chromatography by petroleum ether/dichloromethane to give the desired compound as a white solid (3.50 g, 80 %).

Synthesis of 2-(4-bromophenyl)-5-phenyl-1,3,4-oxadiazole (M3):

4-Bromo-benzoic chloride (3.63 g, 16.5 mmol) in dichloromethane (25 mL) was added dropwise into a solution of benzoyl hydrazine (2.25 g, 16.5 mmol) and triethylamine (3 mL) in dichloromethane (25 mL). The resulting mixture was stirred for 4 h at room temperature and then washed with water. The organic phase separated was evaporated to remove the solvent. Then the solution of the residue in $POCl_3$ was heated at 85℃ for 20 h. After the solvent was removed under reduced pressure, the residue was dissolved into dichloromethane and washed with water. The organic phase separated was dried over $MgSO_4$ and the solvent was evaporated. The crude product was purified by recrystallization from hexane. (4.57 g, 92.0 %).

Synthesis of 2-(4'-(1-(4-(*tert*-butyl)phenyl)-1*H*-phenanthro[9,10-*d*]imidazol-2-yl)-[1,1'-biphenyl]-4-yl)-5-phenyl-1,3,4-oxadiazole (tPPIDPO):

M2 (4.40 g, 7.97 mmol), M3 (2.00 g, 6.64 mmol), potassium carbonate (1.38 g, 9.96 mmol), tetrahydrofuran (50 mL) and deionized water (10 mL), with $Pd(PPh_3)_4$ (0.31 g, 0.27 mmol) acting as catalyst was refluxed at 70 ℃ for 24 h under nitrogen. After the mixture was cooled down, 40 mL deionized water was added to the resulting solution and the mixture was extracted with dichloromethane for several times. The organic phase was dried over anhydrous magnesium sulphate. After filtration and solvent evaporation, the given residue was purified through silica gel column chromatography using ethyl acetate/dichloromethane as eluent to give the product as white solid (3.44 g, 80.0 %). ^{1}H NMR (500 MHz, Chloroform-d) δ 8.90 (d, J = 7.9 Hz, 1H), 8.76 (d, J = 8.5 Hz, 1H), 8.70 (d, J = 8.3 Hz, 1H), 8.17 (td, J = 8.5, 2.1 Hz, 4H), 7.78 – 7.69 (m, 5H), 7.69 – 7.60 (m, 3H), 7.60 – 7.41 (m, 8H), 7.19 (d, J = 8.2 Hz, 1H), 1.47 (s, 9H). ^{13}C NMR (126 MHz, CDCl3) δ 164.64, 164.42, 153.45, 150.24, 143.53, 139.72, 137.52, 136.01, 131.76, 130.52, 129.79, 129.32, 129.10, 128.54, 128.52, 128.31, 127.58, 127.40, 127.29, 127.24, 127.15, 126.97, 126.82, 126.27, 125.63, 124.90, 124.08, 123.94, 123.12, 122.94, 122.74, 120.94, 77.28, 77.02, 76.77, 35.08, 31.44, -0.00. MALDI-TOF MS (mass m/z): calcd for C45H34N4O, 646.2733; found, 647.2812 $[M + H]^+$.

Synthesis of 2-(4'-(3,6-di-*tert*-butyl-9*H*-carbazol-9-yl)-[1,1'-biphenyl]-4-yl)-5-phenyl-1,3,4-oxadiazole (tPCZDPO):

M4 (3.84 g, 6.64 mmol), M3 (2.00 g, 6.64 mmol), potassium carbonate (1.37 g, 9.91 mmol), tetrahydrofuran (50 mL) and deionized water (10 mL), with $Pd(PPh_3)_4$ (0.23 g, 0.20 mmol) acting as catalyst was refluxed at 70 ℃ for 24 h under nitrogen. After the mixture was cooled down, 40 mL deionized water was added to the resulting solution and the mixture was extracted with dichloromethane for several times. The organic phase was dried over anhydrous magnesium sulphate. After filtration and solvent evaporation, the given residue was purified through silica gel column chromatography using ethyl petroleum ether/dichloromethane as eluent to give the product as white solid (3.01 g, 79.0 %). ^{1}H NMR (500 MHz, Chloroform-d) δ 8.33 – 8.25 (m, 2H), 8.22 – 8.12 (m, 4H), 7.88 (d, J = 7.7 Hz, 4H), 7.74 – 7.65 (m, 2H), 7.62 – 7.53 (m, 3H), 7.49 (dd, J = 8.6, 1.9 Hz, 2H), 7.43 (d, J = 8.6 Hz, 2H), 1.48 (s, 18H). ^{13}C NMR (126 MHz, Chloroform-d) δ 164.61 , 143.49 , 143.05 , 138.99 , 138.25 , 138.11 , 131.74 , 129.08 , 128.42 , 127.61 , 127.50 , 126.95 , 123.90 , 123.65 , 123.49 , 122.87 , 116.28 , 109.18 , 34.72 , 31.98. MALDI-TOF MS (mass m/z): calcd for C40H37N3O, 575.2937; found, 575.2938 $[M]^{+}$.

SI-3 Supporting data

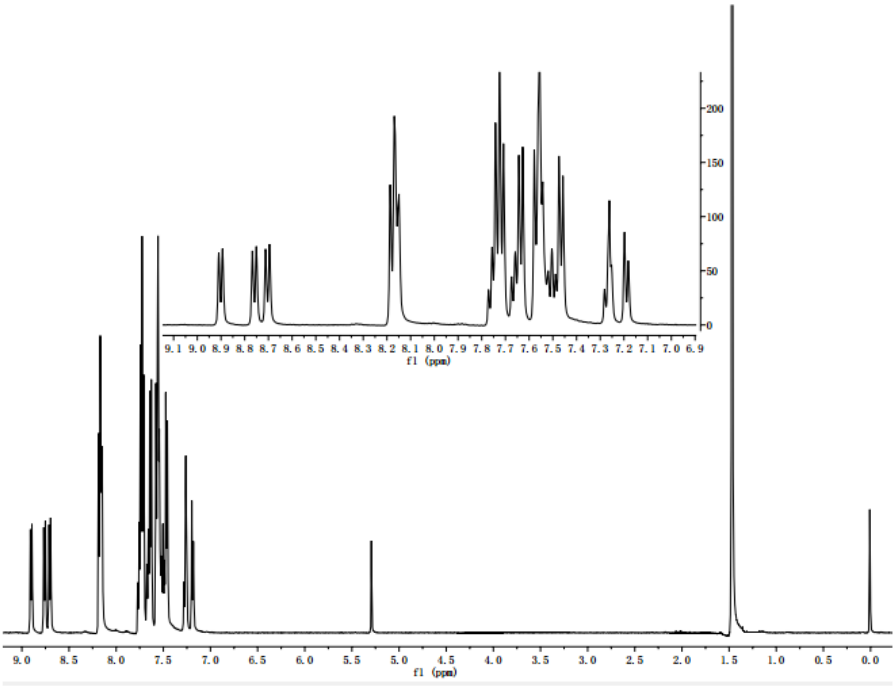

Figure S1. ^{1}H NMR spectrums of tPPIDPO in $CDCl_3$.

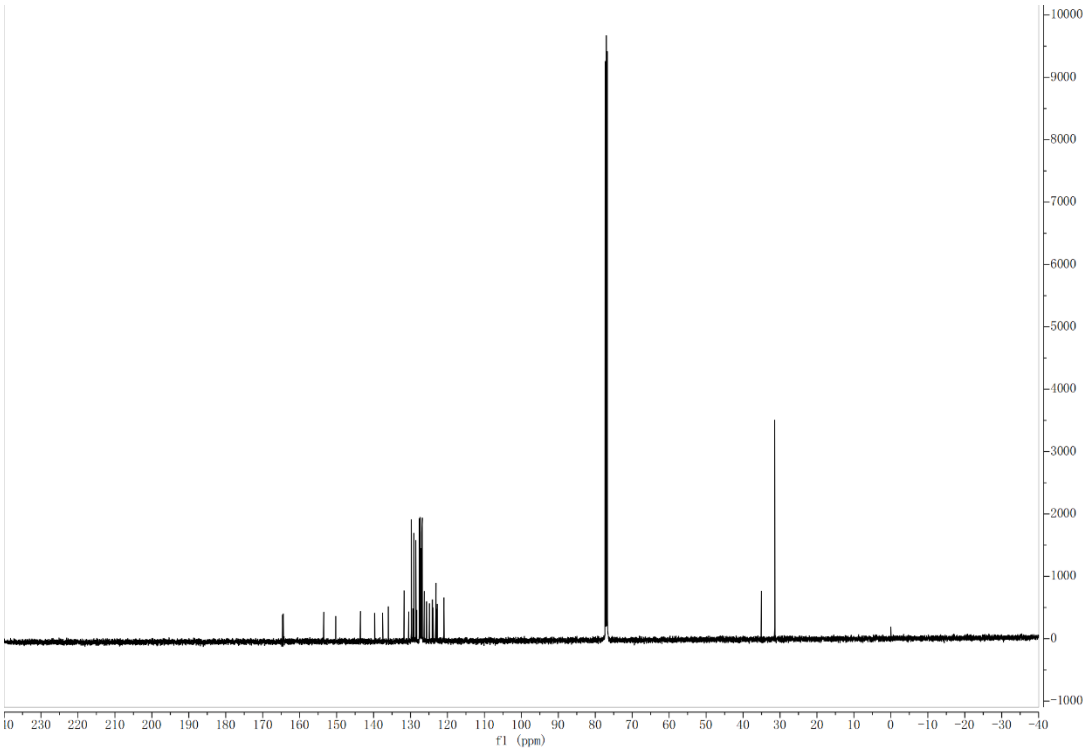

Figure S2. ^{13}C NMR spectrums of tPPIDPO in $CDCl_3$.

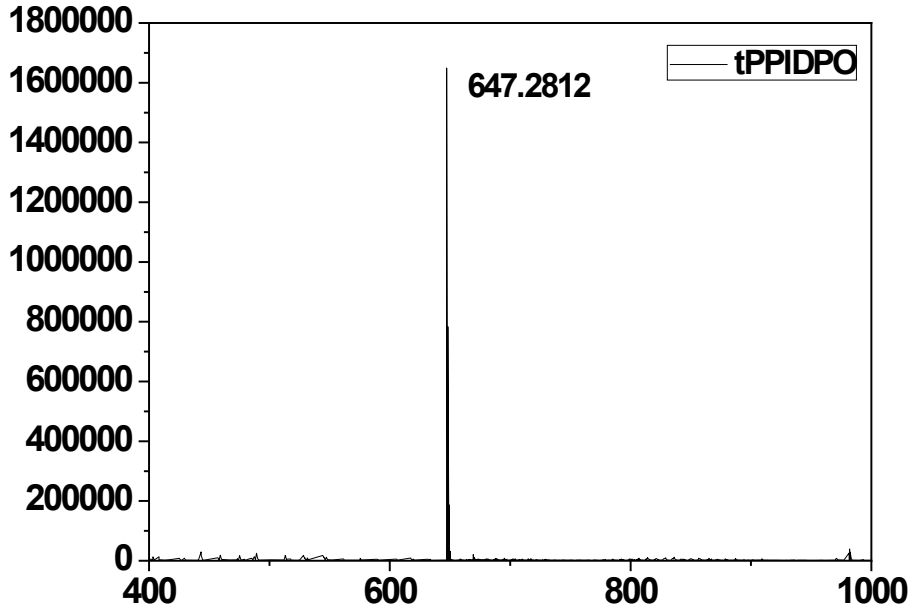

Figure S3. Mass Spectrum $[M + H]^+$ of tPPIDPO.

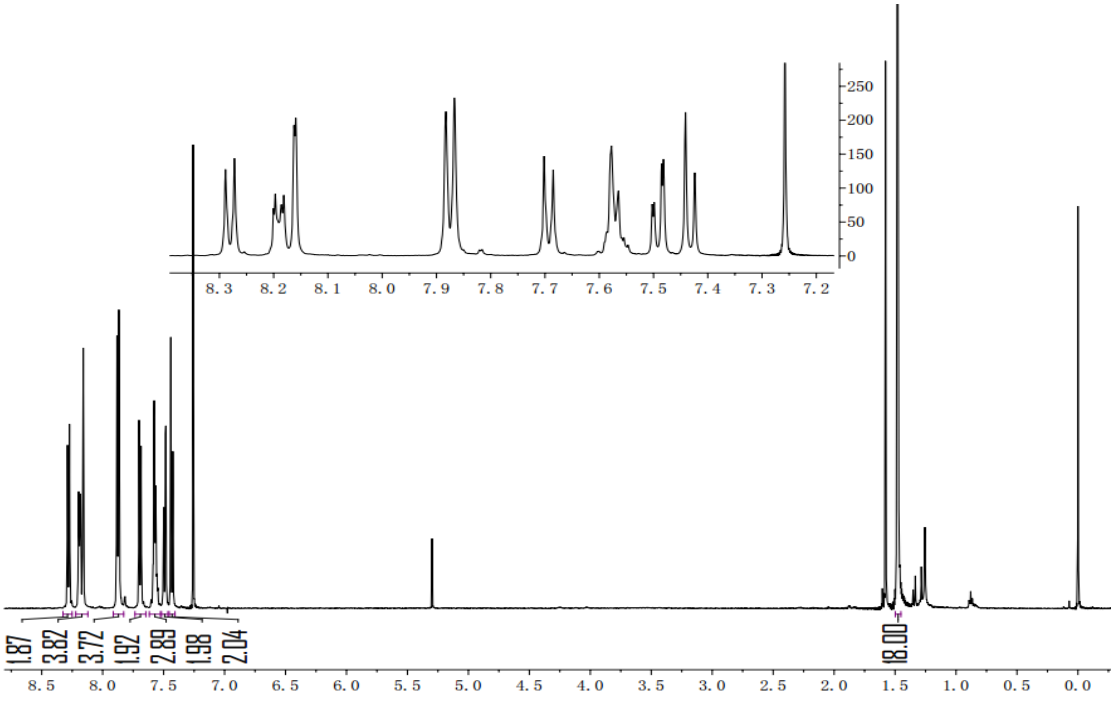

Figure S4. ^1H NMR spectrums of tPCZDPO in $CDCl_3$.

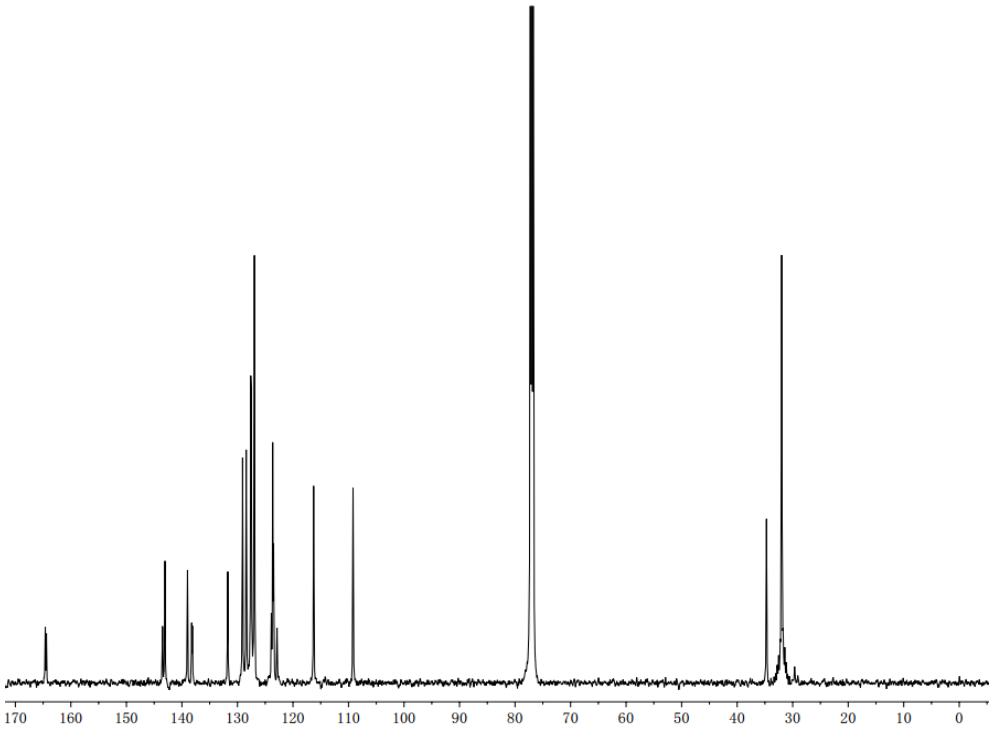

Figure S5. ^{13}C NMR spectrums of tPCZDPO in $CDCl_3$.

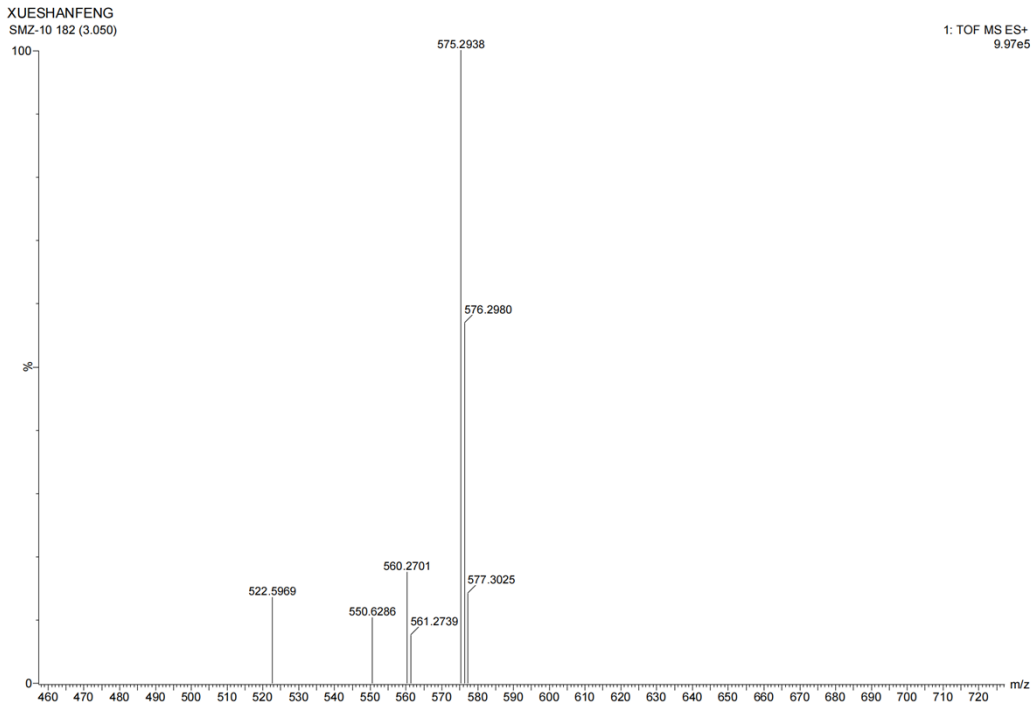

Figure S6. Mass Spectrum $[M]^+$ of tPCZDPO.

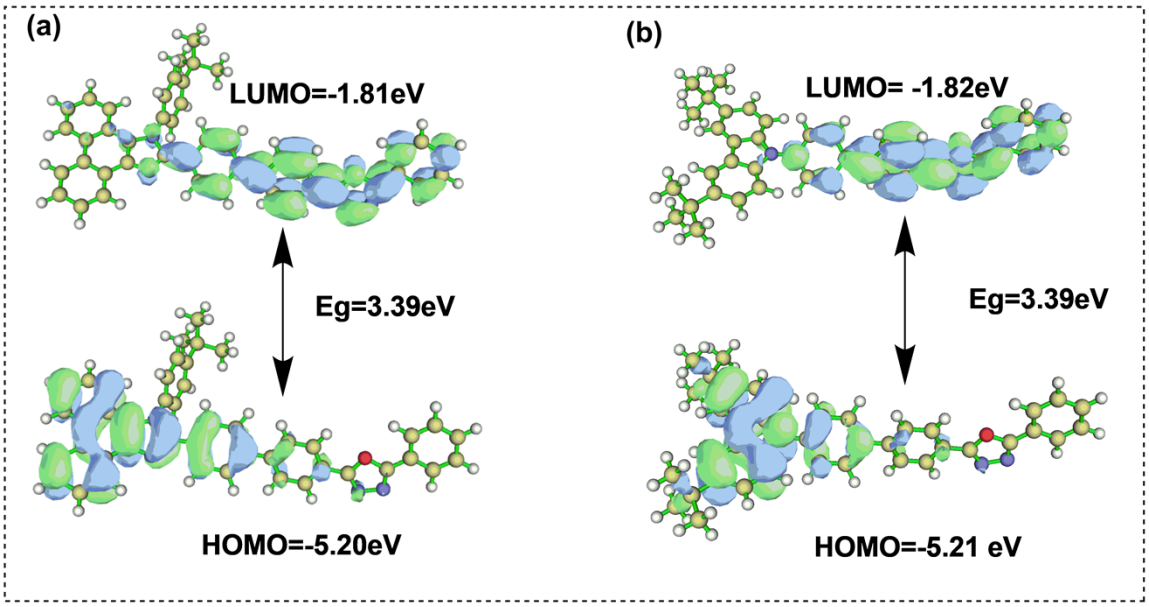

Figure S7. The Frontier Molecular Orbital (FMO) of a) tPPIDPO and b) tPCZDPO.

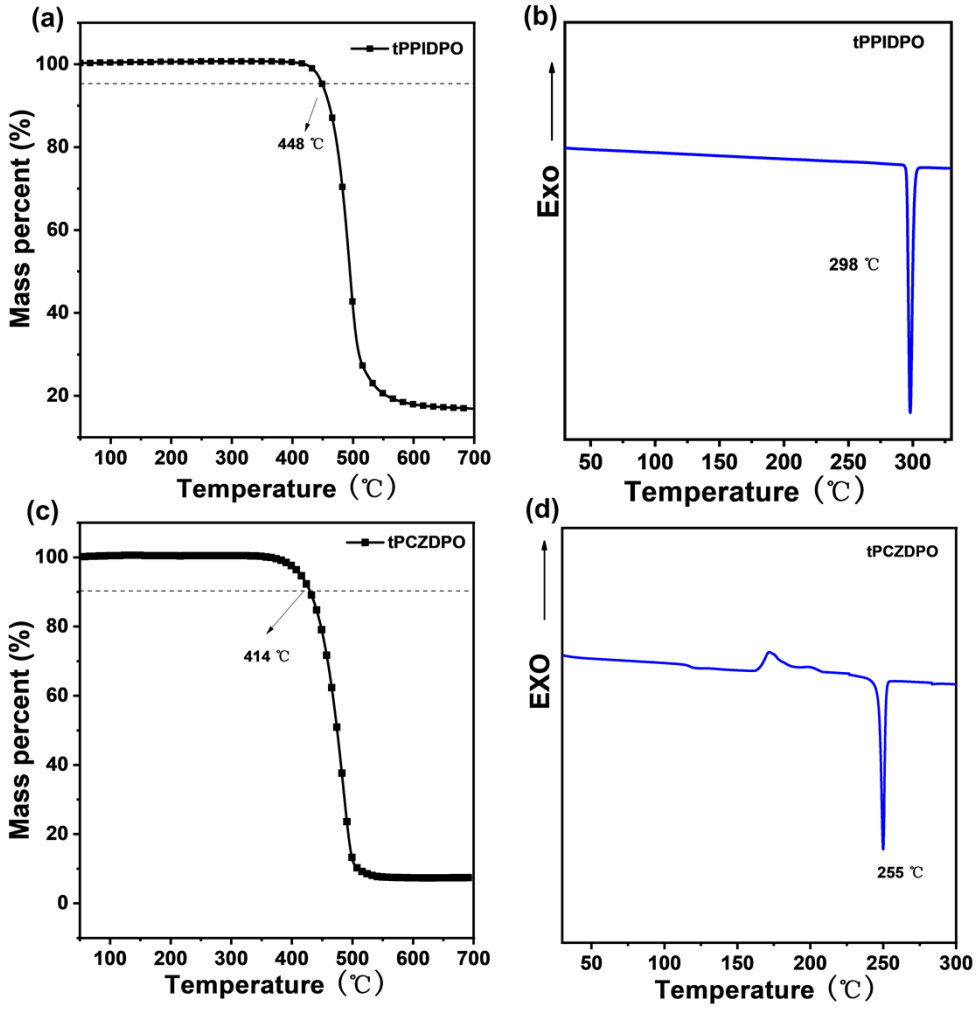

Figure S8. The TGA and DSC graphs of tPPIDPO and tPCZDPO.

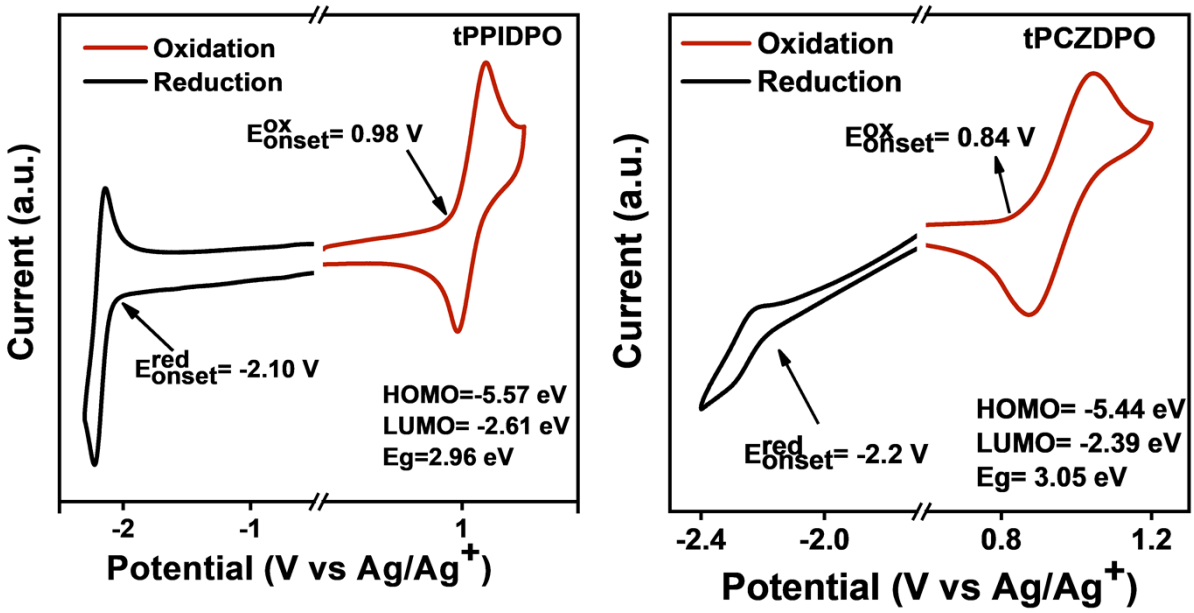

Figure S9. Electrochemical curves of tPPIDPO and tPCZDPO.

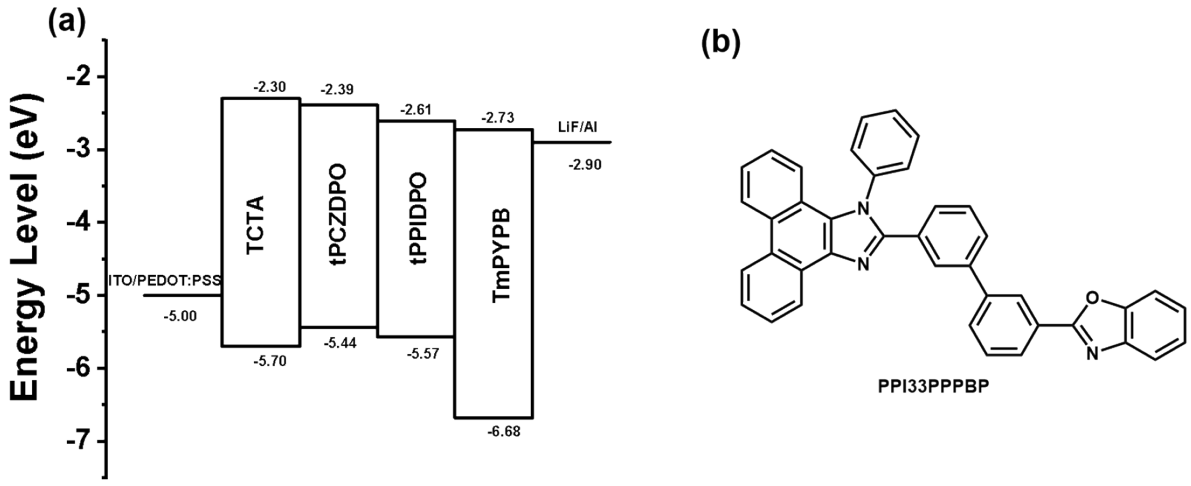

Figure S10. (a) The nondoped device energy level structure diagram. (b) Structural formula of the host PPI33PPPBP.

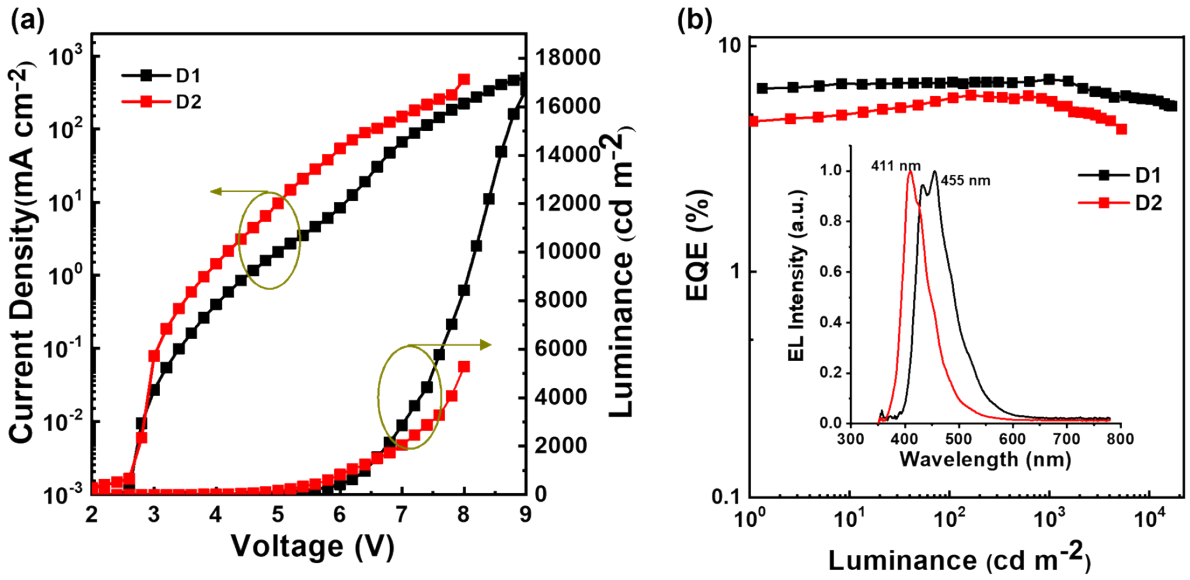

Figure S11. a) Current density-voltage-brightness curves; b) EQE-luminance curves and electroluminescence spectrum of the doped devices N1 and N2.

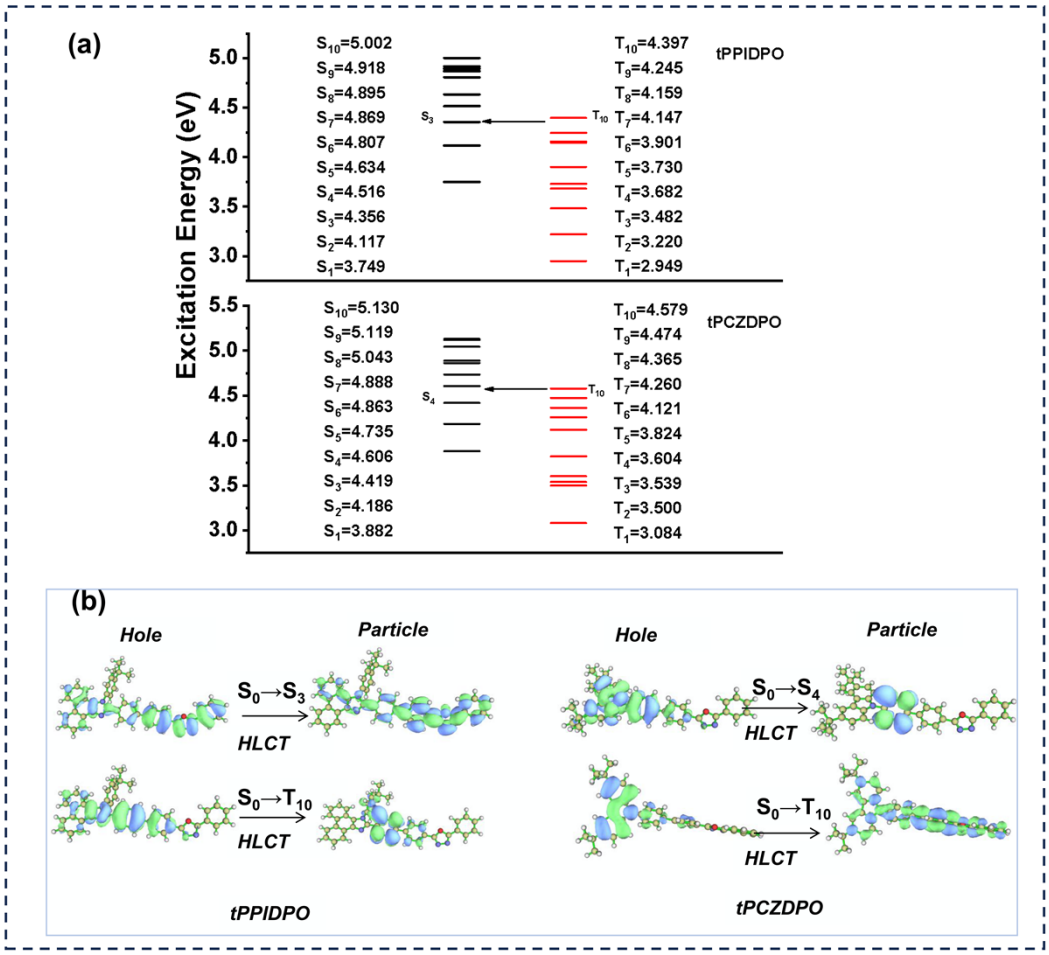

Figure S12 (a) Energy level distribution according to NTOs, (b) the orbital electron cloud distribution of the RISC.

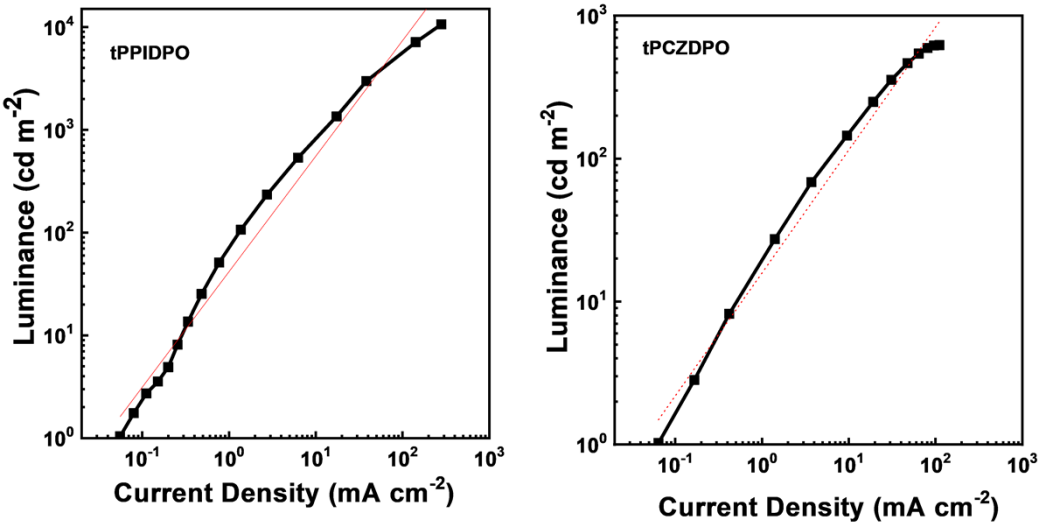

Figure S13. Luminance-current density curves.

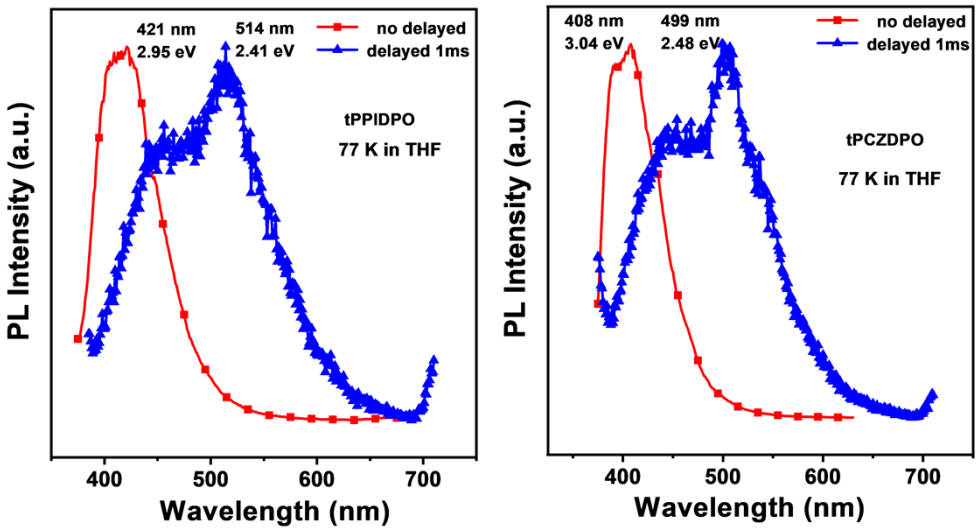

Figure S14. Fluorescence/phosphorescence emission spectrum at 77K in THF.

Table S1. The single crystal data of tPPIDPO.

Compound	tPPIDPO
Chemical formula	C45H25N4O
Formula weight	637.69
Crystal system	triclinic
a/Å	11.6368(17)
b/ Å	b=12.0109(11)

c/ Å	c=14.2329(10)
α/°	88.098(10)
β/°	69.559(11)
γ/°	66.331(11)
Unit cell volume/ Å3	1693.9(8)
Temperature/K	100 K
Space group	P -1
Z	2
Density (calculated) /g cm^{-3}	1.250
F(000)	662.0
Theta range for data collection	2.12 to 24.84
Index ranges	-11<=h<=13, -14<=k<=14, -16<=l<=15
Reflections measured	8188
Independent reflections	1488
Rint	0.0596
Completeness to theta = 72.13°	0.997
Absorption correction	0.076
Max. and min. transmission	0.989 and 0.980
Data / restraints / parameters	5867 / 30 / 463
Goodness-of-fit on F^2	1.049
Final R_1 values ($I> 2\sigma(I)$)	0.0821
Final $wR(F^2)$ values ($I> 2\sigma(I)$)	0.1726
Final R_1values (all data)	0.1488
Final $wR(F^2)$ values (all data)	0.1959
CCDC number	1922590

Table S2. The single crystal data of tPCZDPO.

Compound	tPCZDPO
Chemical formula	C40H37N3O
Formula weight	575.73
Crystal system	monoclinic

a/Å	26.080(11)
b/ Å	b=10.902(5)
c/ Å	c=11.347(5)
α/°	90
β/°	100.628(8)
γ/°	90
Unit cell volume/ Å3	3172(2)
Temperature/K	296 K
Space group	P 21/c
Z	4
Density (calculated) /g cm^{-3}	1.206
F(000)	1224
Theta range for data collection	2.38 to 24.997
Index ranges	-29<=h<=30, -12<=k<=10, -13<=l<=13
Reflections measured	1915
Independent reflections	1488
Rint	0.1132
Completeness to theta = 72.13°	0.997
Absorption correction	0
Max. and min. transmission	0.981 and 0.997
Data / restraints / parameters	5563 /0/ 403
Goodness-of-fit on F^2	1.049
Final R_1 values (I> 2σ(I))	0.0856
Final $wR(F^2)$ values (I> 2σ(I))	0.1895
Final R_1values (all data)	0.1787
Final $wR(F^2)$ values (all data)	0.2226
CCDC number	2281523

Table S3. Thermal performance, photophysical and electrochemical data of tPPIDPO and tPCZDPO.

Compound	λ_{abs} [a)][nm] THF/film	λ_{PL} [b)][nm] THF/film	T_m/T_d [c)] [°C]	HOMO/ LUMO[d)] [eV]	E_g[e)] [eV]	Φ_{PL}[f)] [%] THF/film	τ[g)] film [ns]
tPPIDPO	365/371	449/471	298/448	-5.57/-2.61	2.96	0.93/0.96	2.1
tPCZDPO	347/351	441/435	255/414	-5.44/-2.39	3.95	0.77/0.76	4.1

[a)] UV–vis absorption and [b)] PL value in THF (10^{-5} M) and neat film. [c)] The melting temperature (T_m) and the decomposition temperature (T_d). [d)] The HOMO/LUMO values calculated from the oxidation and reduction peaks measured by CV. [e)] The optical band gap calculated by CV. [f)] The photoluminescence quantum yield in THF and neat films. [g)] The fluorescence lifetime in film state.

Table S4. Absorption and emission peaks in different solvents with different polarities of tPPIDPO and tPCZDPO.

	tPPIDPO	tPCZDPO
	$\lambda_{exmax}/\lambda_{emmax}$ [nm]	$\lambda_{exmax}/\lambda_{emmax}$ [nm]
Hexane	365/407	346/386
Triethylamine	365/410	346/390
Butylether	365/418	346/405
Isopropylether	365/422	346/414
Ethylether	365/436	347/420
Ethylacetate	363/444	345/438
THF	363/447	347/445
Dichloromethane	363/452	346/458
DMF	363/460	346/460
Acetone	363/459	346/469
Acetonitrile	362/468	347/494

Table S5. PLQY of tPPIDPO and tPCZDPO in different solvents with different polarities.

	tPPIDPO [%]	tPCZDPO [%]
hexane	0.63	0.86
Isopropyl ether	0.81	0.83
THF	0.93	0.96
acetonitrile	0.97	0.81

Table S6. Relevant solvents and corresponding detailed data used to draw Stokes curve.

	tPPIDPO	tPCZDPO
	polarization factor (*f*) / stockes shift	polarization factor (*f*) / stockes shift
Hexane	0.0012/2827.235704	0.0012/2994.998353
Butylether	0.096/3473.815298	0.096/4210.376079
Isopropylether	0.145/3700.57781	0.145/4747.144732
Ethylether	0.167/4461.480457	0.167/5092.210295
Ethylacetate	0.2/5025.686844	0.2/6070.683876
THF	0.21/5176.844713	0.21/6429.823992
Dichloromethane	0.217/5424.315561	0.217/7067.672969
Acetone	0.284//5761.716992	0.284/7579.772484
Acetonitrile	0.305/6256.788025	0.305/8658.818124